Since January 2020 Elsevier has created a COVID-19 resource centre with free information in English and Mandarin on the novel coronavirus COVID-19. The COVID-19 resource centre is hosted on Elsevier Connect, the company's public news and information website.

Virus Research 210 (2015) 8–17

Contents lists available at ScienceDirect

Virus Research

journal homepage: www.elsevier.com/locate/virusres

Characterization of self-assembled virus-like particles of dromedary camel hepatitis e virus generated by recombinant baculoviruses

Xianfeng Zhou[a], Michiyo Kataoka[c], Zheng Liu[d], Naokazu Takeda[e], Takaji Wakita[b], Tian-Cheng Li[b,*]

[a] Department of Microbiology, Nanchang Center for Disease Control and Prevention Nanchang, Jiangxi, China
[b] Departments of Virology II, National Institute of Infectious Diseases, Gakuen 4-7-1, Musashi-murayama, Tokyo 208-0011, Japan
[c] Departments of Pathology, National Institute of Infectious Diseases, Gakuen 4-7-1, Musashi-murayama, Tokyo 208-0011, Japan
[d] Department of Biochemistry and Molecular Biophysics, Columbia University, NY, NY 10032, USA
[e] Research Institute for Microbial Diseases, Osaka University, Suita, Osaka 565-0781, Japan

ARTICLE INFO

Article history:
Received 7 April 2015
Received in revised form 26 June 2015
Accepted 30 June 2015
Available online 6 July 2015

Keywords:
Dromedary camel HEV
Recombinant baculovirus
Virus-like particles
VLP
Insect cells Tn5

ABSTRACT

Dromedary camel hepatitis E virus (DcHEV), a novel hepatitis E virus, has been identified in dromedary camels in Dubai, United Arab Emirates. The antigenicity, pathogenicity and epidemiology of this virus have been unclear. Here we first used a recombinant baculovirus expression system to express the 13 and 111 N-terminus amino-acid-truncated DcHEV ORF2 protein in insect Tn5 cells, and we obtained two types of virus-like particles (VLPs) with densities of 1.300 g/cm^3 and 1.285 g/cm^3, respectively. The small VLPs (Dc4sVLPs) were estimated to be 24 nm in diameter, and were assembled by a protein with the molecular mass 53 kDa. The large VLPs (Dc3nVLPs and Dc4nVLPs) were 35 nm in diameter, and were assembled by a 64-kDa protein. An antigenic analysis demonstrated that DcHEV was cross-reactive with G1, G3–G6, ferret and rat HEVs, and DcHEV showed a stronger cross-reactivity to G1 G3–G6 HEV than it did to rat and ferret HEV. In addition, the antibody against DcHEV-LPs neutralized G1 and G3 HEV in a cell culture system, suggesting that the serotypes of these HEVs are identical. We also found that the amino acid residue Met-358 affects the small DcHEV-LPs assembly.

1. Introduction

Hepatitis E virus (HEV) is causative agent of hepatitis E, a viral disease that manifests as acute hepatitis E (Emerson and Purcell, 2003). HEV was named in 1990, when its full genome was identified; before then HEV was identified as "epidemic, non-A, non-B hepatitis" (Reyes et al., 1990; Wong et al., 1980). The HEV infection occurs mainly through the fecal-oral route (Balayan et al., 1983), and acute hepatitis E is known as an important public health problem not only in developing countries but also in industrialized countries, where HEV is transmitted mainly by imported or zoonotic infection (Li et al., 2012; Meng, 2010).

HEV, a small non-enveloped single-stranded positive-sense RNA virus, is classified as the sole member of the genus *Hepevirus* in the family *Hepeviridae* (Meng et al., 2012). The genome of HEV is approximately 7.2 kilo bases (kb) in size, and it contains three open reading frames (ORFs). ORF1 encodes nonstructural proteins involved in replication and viral protein processing. ORF2 both encodes a capsid protein that contains immunogenic epitopes and induces neutralizing antibodies, and ORF2 is the target for vaccine development (Li et al., 2004; Zhu et al., 2010). ORF3, which partially overlaps with ORF2, encodes a cytoskeleton-associated phosphoprotein with multiple functions (Graff et al., 2005; Tyagi et al., 2001, 2004; Zafrullah et al., 1997).

To date, at least four genotypes of HEV that infect humans have been identified. Of the four genotypes of HEV, genotypes 1 and 2 are found exclusively in human beings and are transmitted via contaminated water in developing countries. Genotype 1 occurs mainly in Asia, and genotype 2 occurs mainly in Africa and Mexico. Genotypes 3 and 4 have been isolated from patients as well as from infected animals such as domestic pigs, wild boars and wild deer (Bradley, 1995; Huang et al., 1992; Meng et al., 1997; Takahashi et al., 2002; Zhao et al., 2009). A number of sporadic cases have been transmitted in a zoonotic fashion in developed countries, with zoonotic hepatitis E being mainly associated mainly with genotype 3 or 4 HEV infections (Li et al., 2005; Meng, 2010; Tei et al., 2003).

* Corresponding author at: Department of Virology II, National Institute of Infectious Diseases, 4-7-1 Gakuen Musashi-murayama, Tokyo 208-0011, Japan. Fax: +81 42 565 4729.
E-mail address: litc@nih.go.jp (T.-C. Li).

http://dx.doi.org/10.1016/j.virusres.2015.06.022
0168-1702/

In addition to humans, other animals such as chickens, bats, rats, rabbits, mongooses, foxes, moose, minks, ferrets, and even fish also harbor HEVs, including a number of genetically distant strains (Batts et al., 2011; Bodewes et al., 2013; Drexler et al., 2012; Haqshenas et al., 2001; Jay Lin et al., 2014; Johne et al., 2010; Krog et al., 2013; Nakamura et al., 2006; Raj et al., 2012; Zhao et al., 2009). The division of the *Hepeviridae family* into two genera, *Orthohepevirus* and *Piscihepevirus*, was recently proposed (Smith et al., 2014) (http://ictvonline.org/virusTaxonomy.asp). The orthohepevirus includes four species: *Orthohepevirus A* including isolates from human, pig, wild boar, deer, mongoose, rabbit and camel; *Orthohepevirus B* including isolates from chicken; *Orthohepevirus C* including isolates from rat, greater bandicoot, Asian musk shrew, ferret and mink; and *Orthohepevirus D* including isolates from bat. The cutthroat trout virus belongs to the genus *Piscihepevirus*. Whether these animal HEVs are transmitted to humans is not yet clear, and whether the infected animals develop signs of hepatitis is unknown.

Dromedary camel HEV (DcHEV) was first identified from fecal samples of dromedary camels (*Camelus dromedarius*) in Dubai, United Arab Emirates (Woo et al., 2014). The DcHEV genome is 7.22 kb and contains three major ORFs (OFR1–3). ORF1 encodes a nonstructural protein of 1698 aa, ORF2 encodes a capsid protein of 660 aa, and ORF3 encodes a phosphoprotein of 113 aa. The complete genome sequencing of two DcHEV strains (GenBank accession nos. KJ496143 and KJ496144) showed more than 20% overall nucleotide difference to known HEVs, and only shared 52.1–56.5% nucleotide identity with avian, bat, rat and ferret HEVs (Woo et al., 2014). Though the DcHEV genome has been sequenced, the antigenicity, pathogenicity and epidemiology of DcHEV have remained unclear because of the lack of a cell culture system in which to grow the virus.

Here we describe the efficient expressions of 13- and 111-*N*-terminus-aa-deleted DcHEV ORF2 proteins by a recombinant baculovirus in insect Tn5 cells. The proteins were found to self-assemble into virus-like particles (VLPs). The VLPs exhibited antigenic cross-reactivity with rat, ferret, G1, and G3 to G6 HEVs, and the serotype of DcHEV was identical to those of G1 and G3 HEV.

2. Materials and methods

2.1. Construction of recombinant baculoviruses and the expression of capsid proteins

We synthesized two full-length ORF2s of DcHEV containing the *Bam*HI site before the start codon and the *Xba*I site after the stop codon based on the DcHEV sequences deposited in GenBank (KJ496143 and KJ496144). For simplicity, we propose Dc3 (KJ496143) and Dc4 (KJ496144) as these two DcHEV strains' numbers, respectively. These full-length ORF2s were cloned into a vector, pUC57, to generate the respective plasmids pUC57-Dc3ORF2 and pUC57-Dc4ORF2 (GeneScript, Piscataway, NJ). DNA fragments encoding the N-terminus-truncated DcHEV ORF2s were amplified by polymerase chain reaction (PCR) using plasmid pUC57-Dc3ORF2 or pUC57-Dc4ORF2 as a template.

The DNA fragments encoding 13- and 111-*N*-terminal-aa-truncated DcHEV ORF2s were amplified by PCR with the primers, DcHEV-N13 (5′-AAGGATCCATGTTGCCTATGCTGCCCGCGCCA-3′)/DcHEV-CR1 (5′-AGTCTAGATTAATACTCCCGAGTTTTACCCA-3′) and DcHEV-N111 (5′-AAGGATCCATGGCTGTTGCTCCCGCCCCAGG-3′)/CR1, respectively. The amplified DNA fragments were purified with a Qiagen Gel purification kit (Qiagen, Valencia, CA) and cloned into TA 2.1 cloning vector (Invitrogen, San Diego, CA). The full-length and truncated ORF2s were digested with *Bam*HI and *Xba*I and ligated with the baculovirus transfer vector pVL1393 (Pharmingen, San Diego, CA) to yield plasmids pVL1393Dc3ORF2, pVL1393Dc3n13ORF2, pVL1393Dc3n111ORF2, pVL1393Dc4ORF2, pVL1393Dc4n13ORF2, and pVL1393Dc4n111ORF2.

Mutations were introduced by the PCR amplification of overlapping fragments with specific mutation primers. To introduce the mutation of Thr-358 into Dc3ORF2, we carried out PCR amplifications with primer pairs DcHEV-n111/Dc3ORF2-358R (5′-TAGACCATTCGTACCAGTAAA-3′), and Dc3ORF2-358F (5′-TTTACTGGTACGAATGGTCTA-3′)/CR1, by using the pUC57-Dc3ORF2 as a template. Consequently both fragments were purified and combined in a fusion PCR with the primers DcHEV-n111/CR1. Finally, this fragment was cloned into the transfer vector pVL1393 to yield the plasmid pVL1393Dc3n111ORF2mt. Recombinant viruses were produced in Sf9 cells and designated as Ac[Dc3ORF2], Ac[Dc3n13ORF2], Ac[Dc3n111ORF2], Ac[Dc4ORF2], Ac[Dc4n13ORF2], Ac[Dc4n111ORF2], and Ac[Dc3n111ORF2mt]. To achieve large-scale expression, we used an insect cell line from *Trichoplusia ni* (cabbage looper moth), BTL-Tn 5B1-4 (Tn5) (Invitrogen), infected with recombinant baculoviruses at a multiplicity of infection (MOI) of 10 (Li et al., 1997; Yang et al., 2013).

2.2. SDS-PAGE and Western blot analysis

The proteins in the cell lysates and culture medium were separated by 5–20% sodium dodecyl sulfate-polyacrylamide gel electrophoresis (SDS-PAGE) and detected by Western blot analysis with rabbit anti-G1 HEV-LPs polyclonal antibody as described (Li et al., 1997).

2.3. Purification of VLPs

The recombinant baculovirus-infected Tn5 cells were harvested on day 7 post-infection (p.i.). After the intact cells, cell debris, and progeny baculoviruses were removed by centrifugation at 10,000 *g* for 60 min, the supernatant was spun at 32,000 rpm for 3 h in a Beckman SW32Ti rotor. The resulting pellet was resuspended in EX-cell™ 405 medium at 4 °C overnight. The recombinant baculovirus-infected cells were treated with a denaturation buffer containing 50 mM sodium borate, 150 mM NaCl, 1% Nonidet P-40, 0.5% sodium deoxycholate and 5% 2-mercaptoethanol, and gently rocked at room temperature for 2 h. The lysate was diluted with Ex-cell 405 and centrifuged at 32,000 rpm for 3 h in a Beckman SW32Ti rotor, and the pellet was resuspended in Ex-cell 405 and purified by CsCl gradient centrifugation as described (Li et al., 2007).

2.4. Transmission electron microscopy (TEM)

Purified VLPs were placed on a carbon-coated grid for 45 s, rinsed with distilled water, stained with a 2% uranyl acetate solution and examined with an electron microscope (TEM-1400, JEOL, Tokyo) operating at 80 kV.

2.5. Structural observation

The atomic structure of $T = 1$ particle (PDB-id: 2ztn) and the pseudo-atomic structure of $T = 3$ particle (PDB-id: 3iyo) were both downloaded from the PDB database. The measurements of the distance of residues were performed using Pymol software (http://www.pymol.org), and the figures were made using the software UCSF Chimera (Pettersen et al., 2004).

2.6. N-terminal amino acid sequence analysis

The proteins were purified by CsCl gradient centrifugation. The *N*-terminal aa microsequencing was carried out using 100 pmol of

protein by Edman automated degradation on a protein sequencer Procise 494HT (Applied Biosystems, Carlsbad, CA).

2.7. Hyperimmune sera

We immunized 12-week-old female Wistar rats with Dc3nVLPs. The immunization was initiated as a single thigh muscle injection of purified VLPs at the dose of 200 μg per rat, and booster injections were carried out at 4 and 6 weeks after the first injection with half doses of VLPs. All of the injections, including booster injections, were carried out without any adjuvant. Immunized animals were bled 1 week after the last injection. The Animal Experiment Committee of the National Institute of Infectious Diseases approved this study. All of the animal experiments were reviewed and carried out according to the "Guides for Animal Experiments Performed at the National Institute of Infectious Diseases" under code 114132. The animals were individually housed in BSL-2 facilities.

2.8. Detection of anti-HEV IgG antibody

We performed an enzyme-linked immunosorbent assay (ELISA) for the detection of anti-HEV IgG with purified recombinant HEV-LPs (1 μg/mL, 100 μL/well) (Li et al.,1997, 2000; Yang et al., 2013).

2.9. Neutralizing activity assay

We used the infectious strain G1 (Genbank access no. LC061267) and G3 HEV strain (GenBank access no. AB740232) to evaluate the neutralizing activity of anti-HEVs antibodies. HEV grows in PLC/PRF/5 cells and is efficiently released to cell culture supernatants (Li et al., 2011a). Here we heated pre- and post-HEV-LPs-immunized rat serum and rat HEV-infected rat serum at 56 °C for 30 min and then diluted the sera to 1:10 and 1:100 with medium 199 (Invitrogen). The neutralizing activity assay was carried out as described (Yang et al., 2013). We monitored neutralizing activity by the detection of HEV Ag (capsid protein) in the cell culture supernatant at 3 weeks post-inoculation by ELISA (Li et al., 2004; Yamamoto et al., 2012). The detection of HEV Ag in the culture supernatant indicates that the antibody did not neutralize HEV, whereas the lack of detection of HEV Ag indicates that the antibody has neutralizing activity against HEV.

3. Results

3.1. Expression of DcHEV ORF2 and the formation of VLPs

We prepared six recombinant baculoviruses - Ac[Dc3ORF2], Ac[Dc3n13ORF2], Ac[Dc3n111ORF2], Ac[Dc4ORF2], Ac[Dc4n13ORF2], and Ac[Dc4n111ORF2] – comprising the full-length, and *N*-terminal 13-, and 111-aa-truncated DcHEV ORF2. The proteins generated in the infected cells and supernatant were analyzed by SDS-PAGE. In the Ac[Dc3ORF2] and Ac[Dc4ORF2]-infected Tn5 cells, major protein bands with molecular masses of 72 kDa corresponding to the full-length of ORF2 proteins were detected at 2 days p.i. These proteins were not detected in the supernatant, and no VLPs were observed in the either the cells or their supernatants.

In the Ac[Dc3n111ORF2] and Ac[Dc4n111ORF2]-infected Tn5 cells, a major protein with a molecular mass of 58 kDa (D-p58) was detected in the cells from day 2 p.i., and a protein migrating with a molecular mass of 53 kDa (D-p53) was found in the cells and supernatant from day 4 p.i. The D-p58 protein was synthesized only in Ac[Dc3n111ORF2]- and Ac[Dc4n111ORF2]-infected Tn5 cells, and D-p53 protein was detected only in Ac[Dc3n111ORF2]- and Ac[Dc4n111ORF2]-infected Tn5 cell culture supernatant, not in the mock-infected or wild-type baculovirus-infected cells. The 53-kDa proteins reacted with anti-G1 HEV-LPs antibody in Western blots (Fig. 1).

In a comparison of the amount of D-p53 in supernatant, we found that the D-p53 protein was larger in the Ac[Dc4n111ORF2]-infected cell culture supernatant than that in the Ac[Dc3n111ORF2]-infected cell culture supernatant (Fig. 1). Two small proteins with molecular masses of approximately 17–18 kDa was clearly detected in Ac[Dc3n111ORF2]-infected cell culture supernatant by SDS-PAGE, and these two proteins reacted with rabbit anti-G1 HEV-LPs antibody by Western blotting, indicating that these two proteins were derived from Dc3 ORF2. Although these two proteins were also detected in the Ac[Dc4n111ORF2]-infected cell culture supernatant, their quantities were extremely low. These observed degraded proteins reveal that the D-p53 protein derived from Ac[Dc3n111ORF2] is unstable.

To examine whether the D-p53 protein would form VLPs, we harvested the cell culture supernatants of the Ac[Dc3n111ORF2]- and Ac[Dc4n111ORF2]-infected Tn5 cells at 7 days p.i., and we subjected them to CsCl gradient centrifugation as described in Section 2. In the Ac[Dc4n111ORF2]-infected cell culture supernatant, the D-p53 protein was mainly distributed in fractions 15 and 16, with average densities of 1.285 g/cm^3 ranging from 1.290 g/cm^3 to 1.282 g/cm^3 (Fig. 2A). Electron microscopy (EM) of fractions 15 and 16 showed many spherical particles with a diameter of approximately 24 nm (Fig. 2B), which is similar to those of the G1, G3, G4, ferret and rat HEV-LPs, produced by recombinant baculoviruses harboring *N*-terminal 111 aa-deleted HEV ORF2. Previous cryo-electron microscopic (cryoEM) and crystal structure analyses have revealed that these small HEV-LPs are $T = 1$ icosahedral particles composed of 60 copies of truncated products of ORF2 (Guu et al., 2009; Li et al., 2011b; Xing et al., 2010; Yamashita et al., 2009).

In contrast, the D-p53 protein in Ac[Dc3n111ORF2]-infected Tn5 cell culture supernatant was found in fractions 15 and 16, and some aggregations of D-p53 proteins were observed by EM; however, no VLPs were found (Fig. 2C). We determined the *N*-terminal aa sequence of D-p53 from both Ac[Dc3n111ORF2]- and Ac[Dc4n111ORF2]-infected Tn5 cell culture supernatants by microsequencing, and AVAPA was obtained. This sequence is identical to the 112–116 aa residues of DcHEV ORF2, indicating that D-p53 was derived from the DcHEV ORF2 protein and has an approximately 50-aa deletion at the C-terminus. These results indicate that the D-p53 derived from Dc4 self-assembled into VLPs which are smaller than the native virus particle. We named these particles "Dc4sVLPs." The yield of the purified Dc4sVLPs was 0.1 mg per 10^7 Tn5 cells, which is lower than that of other our previously reported HEV-LPs (Li et al., 1997, 2011b; Yang et al., 2013).

In the Ac[Dc3n13ORF2]- and Ac[Dc4n13ORF2]-infected Tn5 cells, four major proteins with the molecular mass of 40 kDa (p40), 53 kDa (D-p53), 64 kDa (D-p64) and 70 kDa (D-p70) were observed (Fig. 3A). Proteins D-p53, D-p64 and D-p70 were reacted with rabbit anti-G1 HEV-LPs Ab in a Western blot assay, indicating that these three proteins were derived from the DcHEV ORF2. However, the p40 protein did not react with rabbit anti-G1 HEV-LPs antibody. In the cell culture supernatants, only D-p53 was detected by SDS-PAGE (Fig. 3A). To purify VLPs from cells, we harvested Tn5 cells at 7 days p.i. and treated them with denaturing buffer as described in the Section 2. After CsCl gradient centrifugation, proteins, mainly D-p64 appeared in fractions 9 and 10 (Dc3) or fractions 9–11 (Dc4) with average densities of 1.300 g/cm^3 (Fig. 3B). In contrast, a small amount of the D-p53 protein separated in fractions 6-19 (Dc3) or fractions 12 -16 (Dc4). The p40 protein detected in fractions 3 and 4 reacted with anti-TNLC virus antibody by Western blot assay (data not shown) indicating that the p40 protein is the coat protein of TNLC virus, which is a type of nodavirus we ascertained previously (Li et al., 2007).

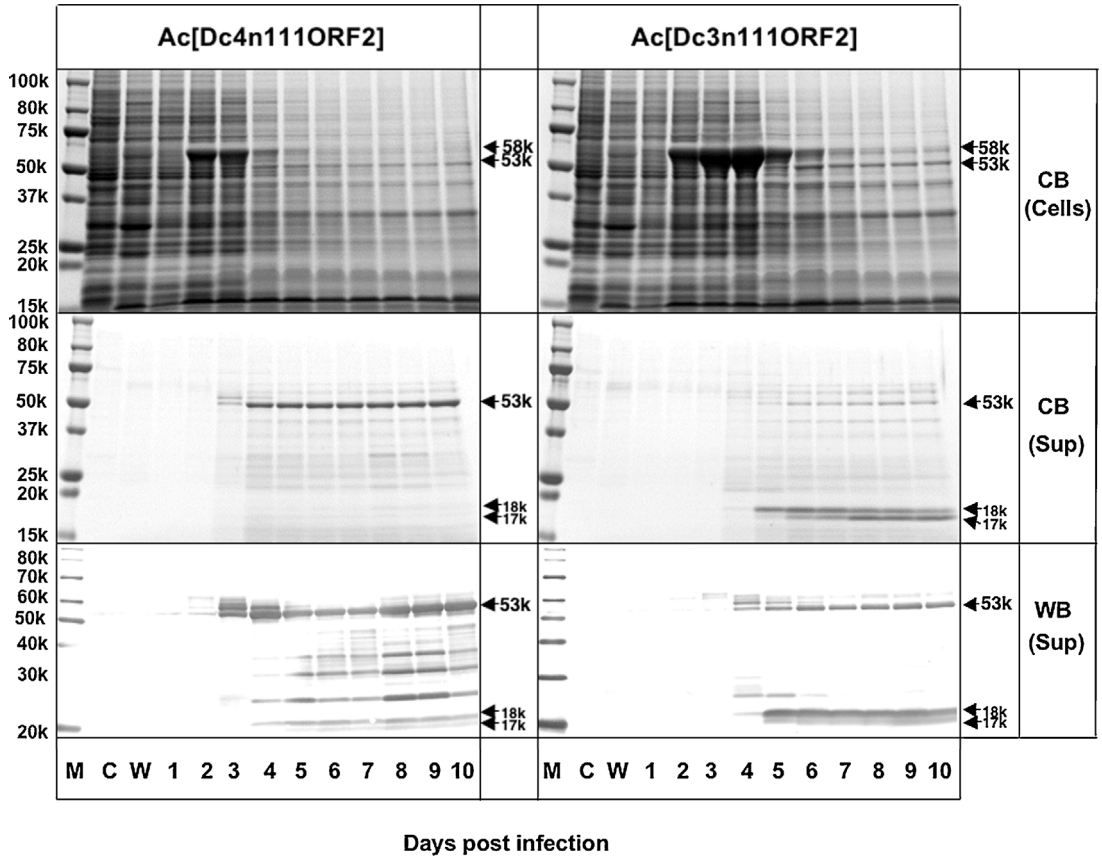

Fig. 1. Time course of the expression of 111-*N*-terminal aa-truncated DcHEV ORF2. Insect Tn5 cells were infected with the recombinant baculovirus Ac[Dc3n111ORF2] or Ac[Dc4n111ORF2], incubated at 26.5 °C, and harvested on the indicated days (days 1–10); then, 5 μL of the culture medium and the lysate from 105 cells were analyzed by SDS-PAGE. Protein bands were visualized by Coomassie blue staining (CB) and a Western blot assay with anti-G1 HEV-LP rabbit serum (WB). M, molecular weight marker; C, mock-infected Tn5 cells; W, wild-type baculovirus-infected Tn5 cells; lanes 1–10, Ac[Dc3n111ORF2]- and Ac[Dc4n111ORF2]-infected Tn5 cells harvested on days 1–10 p.i.

We determined the *N*-terminal aa sequence by microsequencing to identify the D-p64 and LPMLP was obtained. This sequence is identical to that of the 14–18 aa residues of DcHEV ORF2, indicating that D-p64 was derived from the DcHEV ORF2 protein and has an approximately 50-aa deletion at the C-terminus. Our observation of fraction 9 from both Ac[Dc3n13ORF2]- and Ac[Dc4n13ORF2]-infected samples by EM revealed spherical particles with 35-nm diameters (Fig. 3C and D), indicating that the D-p64 protein self-assembled into VLPs. The morphology of these particles is similar to that of the native HEV particle. We named the particles Dc3nVLPs and Dc4nVLPs, respectively.

To determine whether nucleic acids were packaged in these VLPs, we extracted nucleic acids from these purified VLPs and analyzed them on 1% agarose gels. The electrophoresis results demonstrated that both Dc3nVLPs and Dc4nVLPs contained nucleic acids and that they were sensitive to RNase A (data not shown). The next-generation sequence analysis revealed that the nucleic sequence was identical to those of *N*-terminal 13-aa-truncated Dc3 and Dc4HEV ORF2, indicating that the large particles encapsulated the ORF2 genome. The size and density of Dc3nVLPs and Dc4nVLPs were similar to those of the $T=3$ G3 VLPs (Xing et al., 2010). In contrast, no nucleic acid was detected from 24 nm VLPs.

3.2. *The amino acid Met-358 effect* T = *1 DcHEV-LPs formation*

Our comparison of amino acids 111 to 660 between Dc3 and Dc4 ORF2 showed that only two amino acids (aa146 and aa358) were different. In Dc3 and Dc4, the aa146 is Thr and Ser, respectively, and both Ser and Thr in aa146 are common among HEVs in the species *Orthohepevirus* A. The aa358 in Dc3 is Met, and that in Dc4 is Thr. The alignment of the HEV ORF2 amino acid sequence among 242 HEV strains in the species *Orthohepevirus* A revealed that except for rabbit HEV, in only two strains the aa358 is Met and the other aligned sequence is Thr, suggesting that rather than aa146 the Met-358 might be a contributing factor to the abortion of $T=1$ VLPs formation.

To test this hypothesis, we produced a recombinant baculovirus Ac[Dc3n111ORF2mt] comprising a mutated 111-aa-truncated DcHEV ORF2 with the substitution M358T. As shown in Fig. 4, in Ac[Dc3n111ORF2mt]-infected Tn5 cells, similar to Ac[Dc3n111ORF2], a major protein with a molecular mass of 58 kDa was detected in the cells from day 2 p.i., and a protein migrating with a molecular mass of 53 kDa was found in the cells and supernatant from day 4 p.i. However, the amount of D-p53 protein in the Ac[Dc3n111ORF2mt]-infected Tn5 cell culture supernatant was significantly larger than that in Ac[Dc3n111ORF2] and no small proteins (17–18 kDa) were detected. In the CsCl gradient centrifugation, D-p53 appeared mainly in fractions 15–17 with average densities of 1.285 g/cm^3 (Fig. 4B), and the VLPs examined by EM possessed great similarity to the Dc4sVLPs (Fig. 4C). This result indicates that the aa Met-358 affects the formation of $T=1$ VLPs and makes the D-p53 protein unstable.

To further understand how the mutated residue affects the assembly of the expressed proteins into particles, we carefully examined the residue position in both the available atomic model of $T=1$ VLP and the pseudo-model of $T=3$ VLP. In the monomer, the unit constructing the icosahedral particle, the residue is located in a short α-helix situated on top of the long loop, between the B' and C'

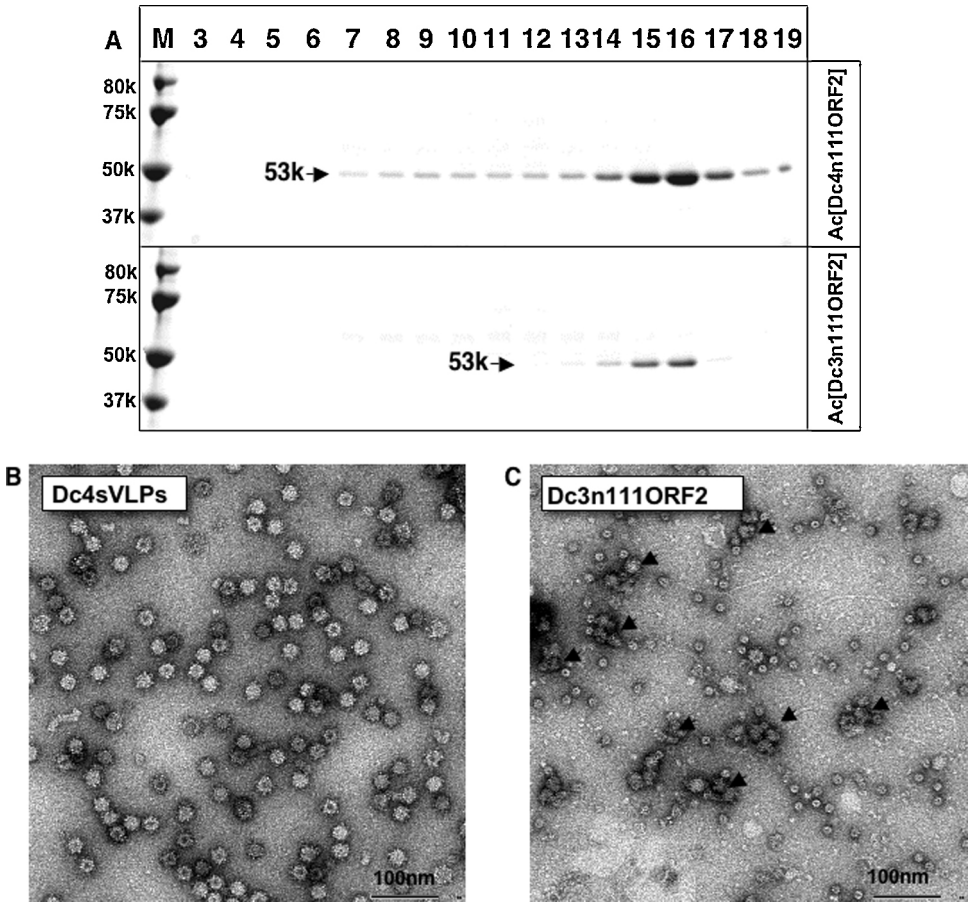

Fig. 2. Purification of VLPs from cell culture. The supernatant of the recombinant baculovirus Ac[Dc3n111ORF2]- and Ac[Dc4n111ORF2]-infected Tn5 cells was centrifuged for 3 h at 32,000 rpm in a Beckman SW32Ti rotor. The pellet was resuspended in 500 μL of EX-cell 405 and then purified by CsCl equilibrium density gradient centrifugation. Aliquots from each fraction were analyzed by electrophoresis on a 5–20% polyacrylamide gel, and CB-stained (A). To examine the VLPs, we stained each fraction containing D-p53 protein with 2% uranyl acetate and observed them by EM: Dc4sVLPs (B) and aggregations of D-p53 proteins (C, arrows). Bar, 100 nm.

strands in the M domain (the nomenclature of secondary structures is according to Yamashita's report; Yamashita et al., 2009) (Fig. 5A).

The aa 358-containing loop is approximately 4 Å from the proline-rich hinge, which serves as a spiller for the propping up of the extending dimeric spikes (P domain) in both $T = 1$ and $T = 3$ VLPs. In $T = 1$ VLP, the aa 358 is mapped on the lateral side of the three-fold protrusions and exposed to solvent (Fig. 5 B). In terms of $T = 3$ VLP, the position of aa 358 differs in the two type dimers: A–B dimer and C–C dimer. In the A–B dimer, aa 358 adopts a position to the side and below the spikes observed from outside of the particle (Fig. 6A and B), and it is right under the P domain in the C–C dimer according to the top view from two-fold axes (Fig. 6C and D).

The alternation of the residue Thr to Met abolishes the presence of a polar hydroxyl (-OH) group with Thr and results in the hydrophobicity yielded by Met. This change may make Met-358 apt to bury itself to avoid solvent and thereby drive its neighboring residues toward three-fold protrusions. Thus, one possibility is that the short α-helix-containing loop may entangle the proline-rich hinge and prevent it from sustaining the spikes, thus resulting in the disruption of extending dimers (spikes) in $T = 1$ VLPs. Given our finding that expressed ORF2 with the mutation from Met-358 back to Thr-358 can assemble into $T = 1$ VLPs again, we confidently propose that the substitution of Thr-358 by Met-358 in the M domain is responsible for the failure of the $T = 1$ VLPs assembly. In the case of the $T = 3$ VLPs, the residue 358, unlike in the $T = 1$ VLPs is not completely exposed to solvent. These residues are positioned to the side and below of the P-domain in the A–B dimer and right under the P-domain in the C–C dimer. Thus, the increase of hydrophobicity of the residues is not able to change their positions significantly in the dimers to affect the regular assembly of $T = 3$ VLPs.

3.3. Antigenic cross-reactivity among ferret, rat, G1, G3–G6 and DcHEVs

Our Western blot analysis results indicated that the DcHEV capsid protein D-p53 reacted with rabbit anti-G1 HEV, suggesting that DcHEV has antigenicity that is similar to that of G1 HEV. To explore the antigenic cross-reactivity among ferret, rat, G1, G3, G4, G5, G6 and DcHEVs, we conducted ELISAs that use Dc3nVLPs as antigen. We detected human anti-G1, G3 and G4 HEV IgG, rat anti-G5 and G6 HEV-LPs IgG, rat anti-rat HEV-IgG, and ferret anti-ferret HEV IgG. We compared the results with that detected by each homologue's antigen.

As shown in Fig. 7A–E, human anti-G1, G3 and G4 HEV IgG, rat anti-G5 and G6 HEV-LPs IgG reacted to Dc3nVLPs and each homologous HEV-LPs with similar titers. In contrast, the titer of rat anti-rat HEV-IgG and ferret anti-ferret HEV IgG detected by using Dc3nVLPs was lower than that detected by homologous HEV-LPs (Fig. 7F and G). These results indicated that DcHEV has antigenic epitope(s) common to those of ferret, rat G1, G3-G6 and DcHEVs, and that the antigenicity of DcHEV is more similar to those of G1 and G3-G6 HEV than rat and ferret HEV.

To obtain antibody against DcHEV, we inoculated a rat with Dc3nVLPs. After three injections, the rat elicited a high level of IgG antibodies against Dc3nVLPs, and the IgG titers reached as high as 1:819,200 by antibody ELISA. The antibody against

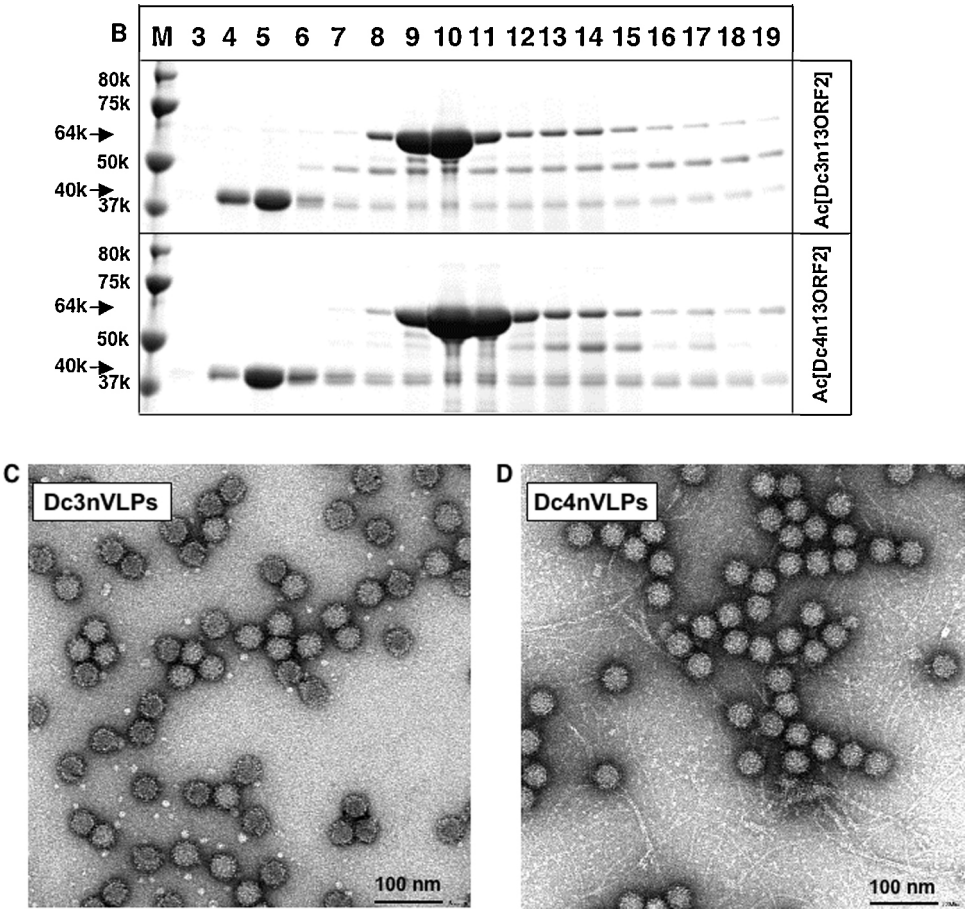

Fig. 3. Expression and purification of VLPs from Ac[Dc3n13ORF2] and Ac[Dc4n13ORF2]-infected Tn5 cells. The time course of the expression of 13-*N*-terminal aa-truncated DcHEV ORF2, protein bands was visualized by Coomassie blue staining (CB) and a Western blot assay with anti-G1 HEV-LP rabbit serum (WB). (A). M, molecular weight marker; C, mock-infected Tn5 cells; W, wild-type baculovirus-infected Tn5 cells; lanes 1 to 10, Ac[Dc3n13ORF2]- and Ac[Dc4n13ORF2]-infected Tn5 cells harvested on days 1–10 p.i. Ac[Dc3n13ORF2]- and Ac[Dc4n13ORF2]-infected Tn5 cells were treated with denaturation buffer as described in Methods, and then purified by CsCl equilibrium density gradient centrifugation. Aliquots from each fraction were analyzed by electrophoresis on a 5–20% polyacrylamide gel, and CB-stained (B). Native size VLPs were observed by EM (C,D). Bar, 100 nm.

Dc3nVLPs reacted not only with Dc3nVLPs but also with heterologous ferret, rat, G1, G3, G4, G5 and G6 HEV-LPs with titers of 1:51,200, 1:102,400, 1: 819,200, 1:819,200, 1:409,600, 1:409,600, and 1:409,600, respectively (Fig. 7H). This result also clearly shows that rat anti-Dc3nVLPs IgG more strongly reacted with G1 and G3–G6 HEV-LPs than with rat and ferret HEV-LPs.

3.4. Cross-neutralization of G1 and G3 HEV with anti-Dc3nHEV-LPs antibodies

To examine the neutralization activity of anti-Dc3nVLPs antibodies, we mixed diluted (1:10 and 1:100) antibodies with G1 and G3 HEV, respectively, incubated the mixture for neutralization, and then inoculated the mixture to PLC/PRF/5 cells. Each pre-immunized rat serum was used as the negative control, and rat anti-G1 and G3 HEV-LPs antiserum was used as the positive control. As shown in Fig. 8, HEV Ag was detected in the samples inoculated with pre-immunized rat serum, with optical density (OD) values ranging from 0.815 to 0.846 (G1) and 0.860 to 1.009 (G3). In contrast, HEV-Ag was not detected in the samples incubated with rat serum against G1, G3 and Dc3nVLPs. These results indicate that G1 and G3 HEV were neutralized by antibody against G1, G3 and Dc3nVLPs. In other words, the serotype of DcHEV is identical to those of the G1 and G3 HEVs.

4. Discussion

The dromedary camel is a new addition to the group of species harboring HEV, and DcHEV was recently proposed as a new genotype of HEV (G7) among *Orthohepevirus* A species with other HEV strains isolated from human, rabbit or wild boar (Smith et al., 2014). Although the DcHEV RNA positive rate was 1.5% in the adult dromedary camel fecal samples, the sero-prevalence is not clear. Because no cell culture system has been developed for DcHEV, it remains necessary to express the capsid protein and generate VLPs in order to analyze the antigenicity and immunogenicity of DcHEV, and to establish a method for the detection of anti-DcHEV IgG and IgM antibodies.

For the production of VLPs in the present study, the full-length ORF2 of Dc3 and Dc4 were initially expressed by a recombinant baculovirus; however, the recombinant protein derived from this gene was not released into the culture supernatant and did not form VLPs. The native size virus-like particles Dc3nVLPs and Dc4nVLPs were obtained by expressing the 13 *N*-terminal aa-truncated Dc3 and Dc4 ORF2. The deletion of 13 *N*-terminal aa and approximately 50*C*-terminal aa does not affect the formation of VLPs. As the native-size VLPs of G3 HEV, nucleic acids were also detected from both Dc3nVLPs and Dc4nVLPs, suggesting that RNA binding might be the extrinsic factor essential for the assembly of HEV native capsid (Xing et al., 2010). Further studies including three-dimensional structural analyses are needed.

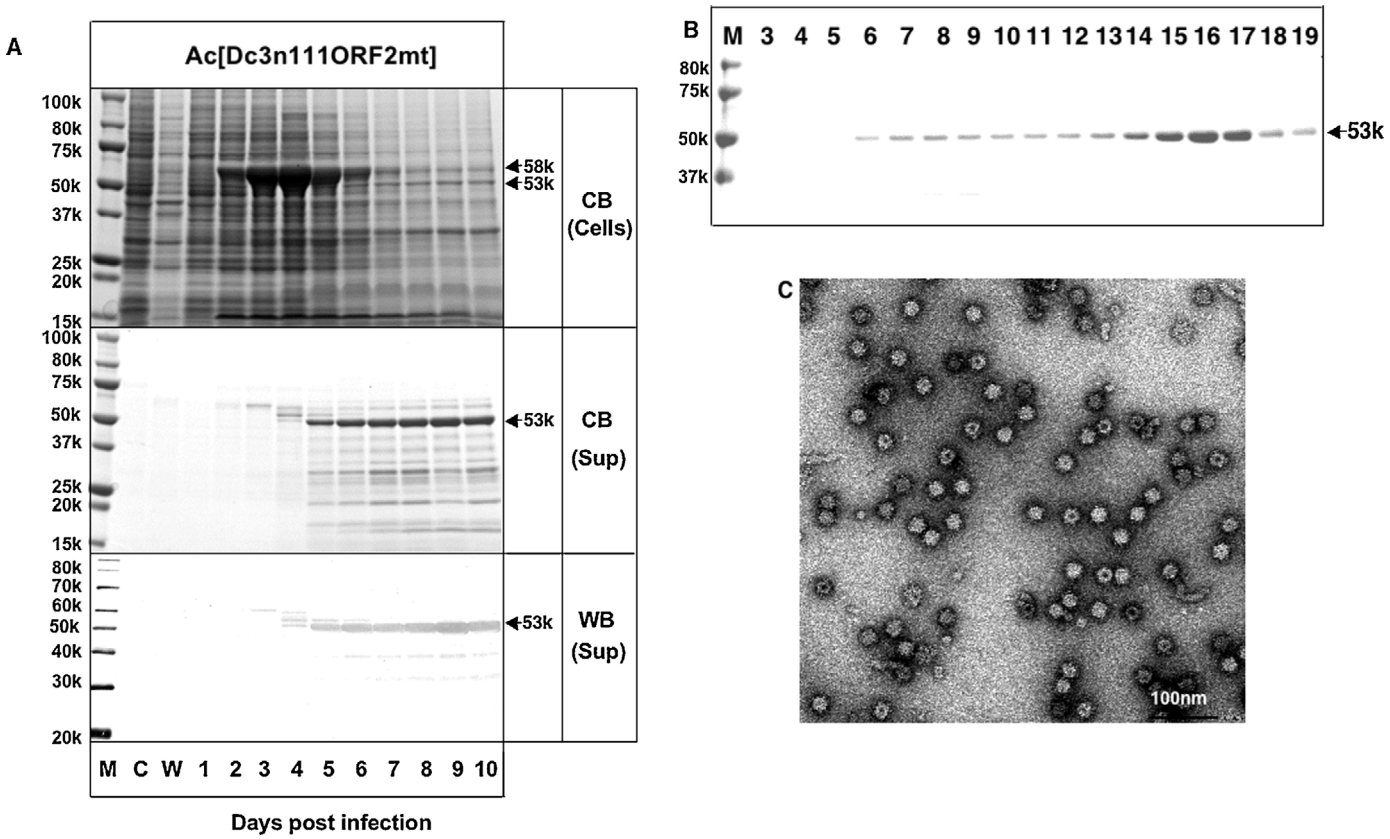

Fig. 4. Expression and purification of VLPs from mutant M358T of 111-*N*-terminal aa-truncated Dc3 ORF2. A mutation of M358T was introduced into Dc3ORF2 and Tn5 cells were infected with a recombinant baculovirus Ac[Dc3n111ORF2mt]. We observed the time course of the expression of the mutant, and protein bands were visualized by CB staining and a Western blot assay with anti-G1 HEV-LP rabbit serum (WB) (A). M, molecular weight marker; C, mock-infected Tn5 cells; W, wild-type baculovirus-infected Tn5 cells; lanes 1–10, Ac[Dc3n111ORF2mt] -infected Tn5 cells harvested on days 1–10 p.i. Proteins in cell culture supernatants were purified by CsCl equilibrium density gradient centrifugation. Aliquots from each fraction were analyzed by electrophoresis on a 5–20% polyacrylamide gel, and CB-stained (B). The VLPs were observed by EM (C). Bar, 100 nm.

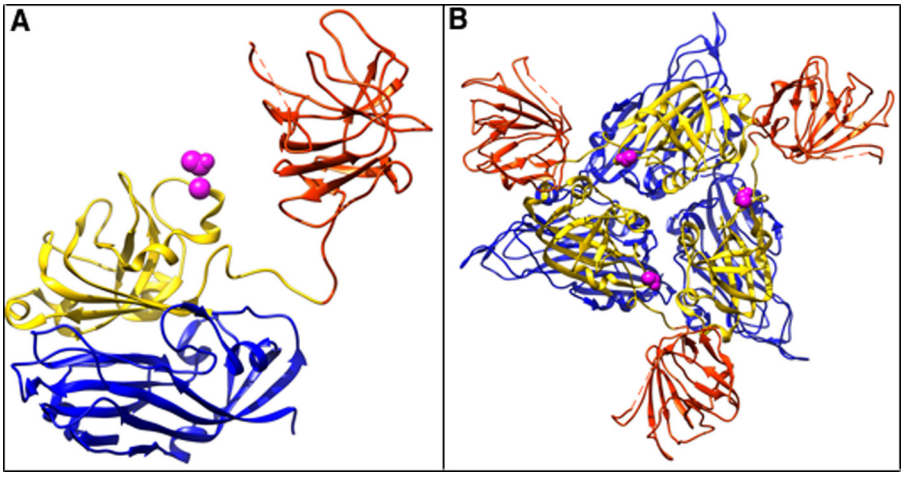

Fig. 5. The Thr-358 in $T = 1$ HEV-LPs capsid. The blue, gold, and orange–red mark the shell (S) domain, the middle (M) domain, and the protruding (P) domain, respectively. Magenta indicates the Thr-358 by sphere for highlighting. Left: Thr-358 localization in the HEV monomer. Right: A trimmer of the capsid protein of HEV-LP viewed from outside of HEV-LP. Three Thr-358s are round the icosahedral 3-fold axes at periphery and exposed to solvent.

The Dc4sVLP was obtained by expressing the *N*-terminal 111-aa deleted Dc4ORF2, which is similar to G1, G3, and G4 HEV. An interesting finding is that a naturally occurring substitution from Thr to Met at aa358 of ORF2 caused the abortion of the small VLPs' assembly. The naturally occurring single point mutation hampers the $T = 1$ particle assembly by the expressed *N*-111 truncated proteins. This phenomenon (i.e., that only one mutation is capable of disrupting the normal assembly of the entire virus particle) was observed with other viruses such as *Sesbania Mosaic virus* (Pappachan et al., 2009), encephalitis virus (Yoshii et al., 2004), nudaurelia capensis ω virus (Taylor and Johnson, 2005), and coronavirus (de Haan et al., 1998).

However, this mutation does not cause disruption of the assembly of $T = 3$ VLPs, which represent the native virions infecting hosts. This result can be explained by the following: in $T = 3$ VLPs, the

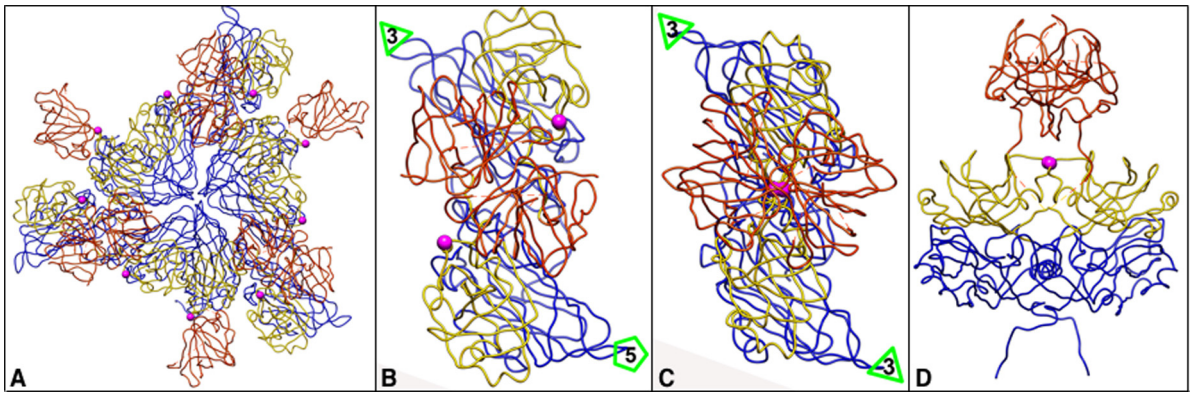

Fig. 6. The aa358 in $T = 3$ HEV-LPs capsid. Magenta indicates the aa358 by sphere for highlighting. The colors used are the same as the colors in Fig. 5. The *S* domains of $T = 3$ VLPs are blue. The triangle and pentagon represent the three-fold axes and five-fold axes, respectively. (A) Thr-358s in a trimer. (B) Thr-358s in an A–B dimer, top view. (C) Thr-358s in a C–C dimer, top view. (D) Thr-358s in a C–C dimer, side view.

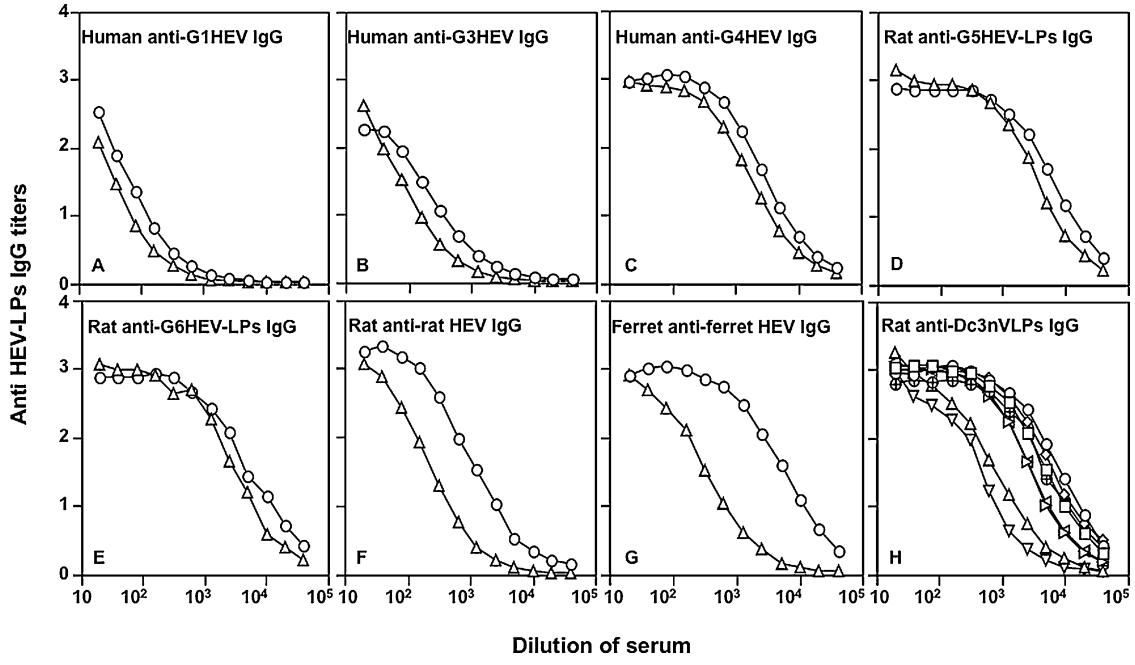

Fig. 7. Antigenic cross-reactivity among ferret, rat, G1, G3–G6 and Dc3nVLPs. A–G: Human anti-G1, G3 and G4 HEV IgG, rat anti-G5 and G6 HEV-LPs IgG, rat anti-rat HEV-IgG, and ferret anti-ferret HEV IgG were detected by ELISA using Dc3nVLPs as antigen (△) and compared with that detected by each homologue's antigen (○). H: The titers of rat anti-Dc3nVLPs IgG were determined by ELISA performed using ferret HEV-LPs (▽), rat HEV-LPs (△), G1 HEV-LPs (□), G3 HEV-LPs (◊), G4 HEV-LPs (⊕), G5 HEV-LPs (▷), G6 HEV-LPs (◁) and Dc3nVLPs (○) as antigen.

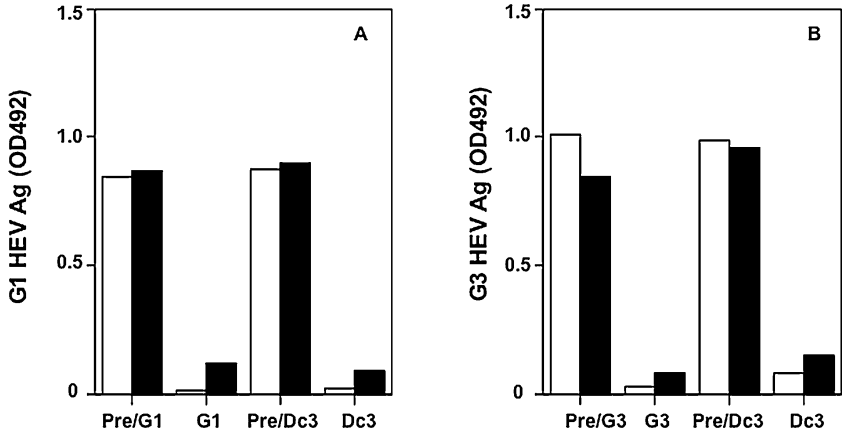

Fig. 8. Neutralizing activity of antibodies against G1 and G3 HEV. The neutralization of G1 HEV (A) and G3 HEV (B) by anti-G1, G3 and Dc3nVLPs sera was carried out by a cell culture-based neutralization test. Bars indicate the OD values of HEV Ag. Pre/G1, Pre/G3 and Pre/Dc3, pre-immunized rat serums; G1, rat anti-G1 HEV-LPs serum; G3, rat anti-G3 HEV-LPs serum; Dc3, rat anti-Dc3nVLPs serum. Rat serum was diluted at 1:10 (white bar) and 1:100 (black bar).

Met-358 is only partially exposed to solvent, which could not yield sufficient force to disrupt the particles' assembly. In light of evolution, this mutation as well should not abort the normal assembly of native forms of DcHEV; otherwise, this strain would not survive in nature.

When rats were immunized with Dc3nVLPs in the present study, a strong immune response was induced with a high IgG titer in the absence of any adjuvant, suggesting that Dc3nVLPs are highly immunogenic. The antibody induced by the Dc3nVLPs was cross-reactive with rat, ferret, G1, and G3–G6 HEV-LPs. These results clearly demonstrated that the DcHEV and rat, ferret, G1, and G3–G6 HEVs share at least one common epitope. The Dc3HEV capsid protein shared higher aa identities (88.5%–91.1%) with G1 and G3–G6 HEVs than did rat and ferret HEVs (56.1–56.7%), and the Dc3nVLPs showed stronger cross-reactivities with anti-G1 and G3–G6 HEV-LP sera.

HEV-LPs are composed of a single capsid protein which folds into three major domains: the shell (S) domain, the middle (M) domain and the protruding (P) domain. The outer surface of the particles, which is a target for antibodies, is formed primarily by the M and P domains (Xing et al., 2010; Yamashita et al., 2009). Although the aa identities of the full-length capsid proteins between Dc3 and rat and ferret HEVs were found to be 56.1% and 56.7%, the amino acid identities of the partial M domains (372–420 aa) and partial P domains (539–567 aa) between Dc3 and rat and ferret HEVs were as high as 83.7% and 75.9%, respectively. These values are both significantly higher than those of the other capsid regions, which suggests that common epitope (s) may be present in the M and/or P domains on the surface of the particles.

We also found that G1 and G3 HEV were neutralized by rat anti-Dc3nVLP antibody, clearly indicating that the serotype of DcHEV is identical to those of G1 and G3 HEVs. Because G1–G4 HEVs have been demonstrated to represent a single serotype (Emerson et al., 2006; Engle et al., 2002), we can conclude that the serotype of DcHEV is identical to that of human HEV.

At present, data other than those describing the nucleotide sequences of the two DcHEV strains from Dubai have not been obtained, including the epidemiology, virology and pathology of this virus. The ELISA based on DcnVLPs for the detection of anti-DcHEV IgG and IgM will be useful for monitoring the circulation of DcHEV in dromedary camels.

Acknowledgments

We thank Sayaka Yoshizaki for the technical assistance. This study was supported in part by grants for Research on Emerging and Re-emerging Infectious Diseases, for Research on Hepatitis from the Ministry of Health, Labour, and Welfare of Japan (No. 25181501). Xianfeng Zhou was supported by the Japan-China Sasagawa Medical Fellowship, funded by the Japan-China Medical Association and The Nippon Foundation.

References

Balayan, M.S., Andjaparidze, A.G., Savinskaya, S.S., Ketiladze, E.S., Braginsky, D.M., Savinov, A.P., Poleschuk, V.F., 1983. Evidence for a virus in non-A, non-B hepatitis transmitted via the fecal-oral route. Intervirology 20, 23–31.

Batts, W., Yun, S., Hedrick, R., Winton, J., 2011. A novel member of the family Hepeviridae from cutthroat trout (Oncorhynchus clarkii). Virus Res 158, 116–123.

Bodewes, R., van der Giessen, J., Haagmans, B.L., Osterhaus, A.D., Smits, S.L., 2013. Identification of multiple novel viruses, including a parvovirus and a hepevirus, in feces of red foxes. J. Virol. 87, 7758–7764.

Bradley, D.W., 1995. Hepatitis E virus: a brief review of the biology, molecular virology, and immunology of a novel virus. J. Hepatol. 22, 140–145.

de Haan, C.A., Kuo, L., Masters, P.S., Vennema, H., Rottier, P.J., 1998. Coronavirus particle assembly: primary structure requirements of the membrane protein. J. Virol. 72, 6838–6850.

Drexler, J.F., Seelen, A., Corman, V.M., Fumie Tateno, A., Cottontail, V., Melim Zerbinati, R., Gloza-Rausch, F., Klose, S.M., Adu-Sarkodie, Y., Oppong, S.K., Kalko, E.K., Osterman, A., Rasche, A., Adam, A., Muller, M.A., Ulrich, R.G., Leroy, E.M., Lukashev, A.N., Drosten, C., 2012. Bats worldwide carry hepatitis E virus-related viruses that form a putative novel genus within the family Hepeviridae. J. Virol. 86, 9134–9147.

Emerson, S.U., Clemente-Casares, P., Moiduddin, N., Arankalle, V.A., Torian, U., Purcell, R.H., 2006. Putative neutralization epitopes and broad cross-genotype neutralization of Hepatitis E virus confirmed by a quantitative cell-culture assay. J. Gen. Virol. 87, 697–704.

Emerson, S.U., Purcell, R.H., 2003. Hepatitis E virus. Rev. Med. Virol. 13, 145–154.

Engle, R.E., Yu, C., Emerson, S.U., Meng, X.J., Purcell, R.H., 2002. Hepatitis E virus (HEV) capsid antigens derived from viruses of human and swine origin are equally efficient for detecting anti-HEV by enzyme immunoassay. J. Clin. Microbiol. 40, 4576–4580.

Graff, J., Nguyen, H., Yu, C., Elkins, W.R., St Claire, M., Purcell, R.H., Emerson, S.U., 2005. The open reading frame 3 gene of hepatitis E virus contains a cis-reactive element and encodes a protein required for infection of macaques. J. Virol. 79, 6680–6689.

Guu, T.S., Liu, Z., Ye, Q., Mata, D.A., Li, K., Yin, C., Zhang, J., Tao, Y.J., 2009. Structure of the hepatitis E virus-like particle suggests mechanisms for virus assembly and receptor binding. Proc. Natl. Acad. Sci. U. S. A. 106, 12992–12997.

Haqshenas, G., Shivaprasad, H.L., Woolcock, P.R., Read, D.H., Meng, X.J., 2001. Genetic identification and characterization of a novel virus related to human hepatitis E virus from chickens with hepatitis-splenomegaly syndrome in the United States. J. Gen. Virol. 82, 2449–2462.

Huang, C.C., Nguyen, D., Fernandez, J., Yun, K.Y., Fry, K.E., Bradley, D.W., Tam, A.W., Reyes, G.R., 1992. Molecular cloning and sequencing of the Mexico isolate of hepatitis E virus (HEV). Virology 191, 550–558.

Jay Lin, Heléne Norder, Henrik Uhlhorn, Sándor Belák, Widén, F., 2014. Novel hepatitis E like virus found in Swedish moose. J. Gen. Virol. 95 (Pt 3), 557–570.

Johne, R., Heckel, G., Plenge-Bönig, A., Kindler, E., Maresch, C., Reetz, J., Schielke, A., Ulrich, R.G., 2010. Novel hepatitis E virus genotype in Norway rats, Germany. Emerg. Infect. Dis. 16, 1452–1455.

Krog, J.S., Breum, S.O., Jensen, T.H., Larsen, L.E., 2013. Hepatitis E virus variant in farmed mink, Denmark. Emerg. Infect. Dis. 19, 2028–2030.

Li, T.-C., Song, S., Yang, Q., Ishii, K., Takeda, N., Wakita, T., 2011a. The stability and inactivation of hepatitis E virus grows in cell culture. Hepatology International 5, 202.

Li, T.C., Chijiwa, K., Sera, N., Ishibashi, T., Etoh, Y., Shinohara, Y., Kurata, Y., Ishida, M., Sakamoto, S., Takeda, N., Miyamura, T., 2005. Hepatitis E virus transmission from wild boar meat. Emerg Infect Dis 11, 1958–1960.

Li, T.C., Ochiai, S., Ishiko, H., Wakita, T., Miyamura, T., Takeda, N., 2012. A retrospective study on imported hepatitis E in Japan. Travel Med Infect Dis 10, 80–85.

Li, T.C., Scotti, P.D., Miyamura, T., Takeda, N., 2007. Latent infection of a new alphanodavirus in an insect cell line. J. Virol 81, 10890–10896.

Li, T.C., Suzaki, Y., Ami, Y., Dhole, T.N., Miyamura, T., Takeda, N., 2004. Protection of cynomolgus monkeys against HEV infection by oral administration of recombinant hepatitis E virus-like particles. Vaccine 22, 370–377.

Li, T.C., Yamakawa, Y., Suzuki, K., Tatsumi, M., Razak, M.A., Uchida, T., Takeda, N., Miyamura, T., 1997. Expression and self-assembly of empty virus-like particles of hepatitis E virus. J. Virol. 71, 7207–7213.

Li, T.C., Yoshimatsu, K., Yasuda, S.P., Arikawa, J., Koma, T., Kataoka, M., Ami, Y., Suzaki, Y., Mai le, T.Q., Hoa, N.T., Yamashiro, T., Hasebe, F., Takeda, N., Wakita, T., 2011b. Characterization of self-assembled virus-like particles of rat hepatitis E virus generated by recombinant baculoviruses. J. Gen. Virol. 92, 2830–2837.

Li, T.C., Zhang, J., Shinzawa, H., Ishibashi, M., Sata, M., Mast, E.E., Kim, K., Miyamura, T., Takeda, N., 2000. Empty virus-like particle-based enzyme-linked immunosorbent assay for antibodies to hepatitis E virus. J. Med. Virol. 62, 327–333.

Meng, X.J., 2010. Hepatitis E virus: animal reservoirs and zoonotic risk. Vet. Microbiol. 140, 256–265.

Meng, X.J., Anderson, D.A., Arankalle, V.A., Emerson, S.U., Harrison, T.J., Jameel, S., Okamoto, H., 2012. Hepeviridae. In: King, A.M.Q.A., Adams, M.J., Carstens, E.B., Lefkowitz, E.J. (Eds.), Virus Taxonomy: Ninth Report of the ICTV. Elsevier/Academic Press, London, pp. 1021–1028.

Meng, X.J., Purcell, R.H., Halbur, P.G., Lehman, J.R., Webb, D.M., Tsareva, T.S., Haynes, J.S., Thacker, B.J., Emerson, S.U., 1997. A novel virus in swine is closely related to the human hepatitis E virus. Proc. Natl. Acad. Sci. U. S. A. 94, 9860–9865.

Nakamura, M., Takahashi, K., Taira, K., Taira, M., Ohno, A., Sakugawa, H., Arai, M., Mishiro, S., 2006. Hepatitis E virus infection in wild mongooses of Okinawa, Japan: demonstration of anti-HEV antibodies and a full-genome nucleotide sequence. Hepatol. Res. 34, 137–140.

Pappachan, A., Chinnathambi, S., Satheshkumar, P.S., Savithri, H.S., Murthy, M.R., 2009. A single point mutation disrupts the capsid assembly in Sesbania Mosaic Virus resulting in a stable isolated dimer. Virology 392, 215–221.

Pettersen, E.F., Goddard, T.D., Huang, C.C., Couch, G.S., Greenblatt, D.M., Meng, E.C., Ferrin, T.E., 2004. UCSF Chimera–a visualization system for exploratory research and analysis. J. Comput. Chem. 25, 1605–1612.

Raj, V.S., Smits, S.L., Pas, S.D., Provacia, L.B., Moorman-Roest, H., Osterhaus, A.D., Haagmans, B.L., 2012. Novel hepatitis e virus in ferrets, the Netherlands. Emerg. Infect. Dis. 18, 1369–1370.

Reyes, G.R., Purdy, M.A., Kim, J.P., Luk, K.C., Young, L.M., Fry, K.E., Bradley, D.W., 1990. Isolation of a cDNA from the virus responsible for enterically transmitted non-A, non-B hepatitis. Science 247, 1335–1339.

Smith, D.B., Simmonds, P., Jameel, S., Emerson, S.U., Harrison, T.J., Meng, X.J., Okamoto, H., Van der Poel, W.H., Purdy, M.A., 2014. Consensus proposals for classification of the family Hepeviridae. J. Gen. Virol. 95, 2223–2232.

Takahashi, M., Nishizawa, T., Yoshikawa, A., Sato, S., Isoda, N., Ido, K., Sugano, K., Okamoto, H., 2002. Identification of two distinct genotypes of hepatitis E virus in a Japanese patient with acute hepatitis who had not travelled abroad. J. Gen. Virol. 83, 1931–1940.

Taylor, D.J., Johnson, J.E., 2005. Folding and particle assembly are disrupted by single-point mutations near the autocatalytic cleavage site of Nudaurelia capensis omega virus capsid protein. Protein Sci. 14, 401–408.

Tei, S., Kitajima, N., Takahashi, K., Mishiro, S., 2003. Zoonotic transmission of hepatitis E virus from deer to human beings. Lancet 362, 371–373.

Tyagi, S., Jameel, S., Lal, S.K., 2001. Self-association and mapping of the interaction domain of hepatitis E virus ORF3 protein. J. Virol. 75, 2493–2498.

Tyagi, S., Surjit, M., Roy, A.K., Jameel, S., Lal, S.K., 2004. The ORF3 protein of hepatitis E virus interacts with liver-specific alpha1-microglobulin and its precursor alpha1-microglobulin/bikunin precursor (AMBP) and expedites their export from the hepatocyte. J. Biol. Chem. 279, 29308–29319.

Wong, D.C., Purcell, R.H., Sreenivasan, M.A., Prasad, S.R., Pavri, K.M., 1980. Epidemic and endemic hepatitis in India: evidence for a non-A, non-B hepatitis virus aetiology. Lancet 2, 876–879.

Woo, P.C., Lau, S.K., Teng, J.L., Tsang, A.K., Joseph, M., Wong, E.Y., Tang, Y., Sivakumar, S., Xie, J., Bai, R., Wernery, R., Wernery, U., Yuen, K.Y., 2014. New hepatitis E virus genotype in camels, the Middle East. Emerg. Infect. Dis. 20, 1044–1048.

Xing, L., Li, T.C., Mayazaki, N., Simon, M.N., Wall, J.S., Moore, M., Wang, C.Y., Takeda, N., Wakita, T., Miyamura, T., Cheng, R.H., 2010. Structure of hepatitis E virion-sized particle reveals an RNA-dependent viral assembly pathway. J. Biol. Chem. 285, 33175–33183.

Yamamoto, H., Suzuki, J., Matsuda, A., Ishida, T., Ami, Y., Suzaki, Y., Adachi, I., Wakita, T., Takeda, N., Li, T.C., 2012. Hepatitis e virus outbreak in monkey facility, Japan. Emerg. Infect. Dis. 18, 2032–2034.

Yamashita, T., Mori, Y., Miyazaki, N., Cheng, R.H., Yoshimura, M., Unno, H., Shima, R., Moriishi, K., Tsukihara, T., Li, T.C., Takeda, N., Miyamura, T., Matsuura, Y., 2009. Biological and immunological characteristics of hepatitis E virus-like particles based on the crystal structure. Proc. Natl. Acad. Sci. U. S. A. 106, 12986–12991.

Yang, T., Kataoka, M., Ami, Y., Suzaki, Y., Kishida, N., Shirakura, M., Imai, M., Asanuma, H., Takeda, N., Wakita, T., Li, T.C., 2013. Characterization of self-assembled virus-like particles of ferret hepatitis E virus generated by recombinant baculoviruses. J. Gen. Virol. 94, 2647–2656, Pt 12.

Yoshii, K., Konno, A., Goto, A., Nio, J., Obara, M., Ueki, T., Hayasaka, D., Mizutani, T., Kariwa, H., Takashima, I., 2004. Single point mutation in tick-borne encephalitis virus prM protein induces a reduction of virus particle secretion. J. Gen. Virol. 85, 3049–3058.

Zafrullah, M., Ozdener, M.H., Panda, S.K., Jameel, S., 1997. The ORF3 protein of hepatitis E virus is a phosphoprotein that associates with the cytoskeleton. J. Virol. 71, 9045–9053.

Zhao, C., Ma, Z., Harrison, T.J., Feng, R., Zhang, C., Qiao, Z., Fan, J., Ma, H., Li, M., Song, A., Wang, Y., 2009. A novel genotype of hepatitis E virus prevalent among farmed rabbits in China. J. Med. Virol. 81, 1371–1379.

Zhu, F.C., Zhang, J., Zhang, X.F., Zhou, C., Wang, Z.Z., Huang, S.J., Wang, H., Yang, C.L., Jiang, H.M., Cai, J.P., Wang, Y.J., Ai, X., Hu, Y.M., Tang, Q., Yao, X., Yan, Q., Xian, Y.L., Wu, T., Li, Y.M., Miao, J., Ng, M.H., Shih, J.W., Xia, N.S., 2010. Efficacy and safety of a recombinant hepatitis E vaccine in healthy adults: a large-scale, randomised, double-blind placebo-controlled, phase 3 trial. Lancet 376, 895–902.